

The feasibility of monitoring CO₂ from high resolution infrared sounders

A. Chedin¹, A. Hollingsworth², N. Scott¹,
R. Saunders^{2*}, M. Matricardi², J. Etcheto³,
C. Clerbaux⁴, R. Armante¹

Research Department

Affiliations:

1. Laboratoire de Météorologie Dynamique, École Polytechnique, Palaiseau, France
2. European Centre for Medium-Range Weather Forecasting, Shinfield Park, Reading U.K.
3. Laboratoire d'Océanographie Dynamique et de Climatologie, Université Pierre et Marie Curie, Paris, France
4. Service d'Aéronomie, Université de Paris 6, Paris, France

November 2001
Submitted to J.Geophys.Res.

For additional copies please contact

The Library
ECMWF
Shinfield Park
Reading, Berks RG2 9AX

library@ecmwf.int

Series: ECMWF Technical Memoranda

A full list of ECMWF Publications can be found on our web site under:
<http://www.ecmwf.int/pressroom/publications.html>

© Copyright 2001

European Centre for Medium Range Weather Forecasts
Shinfield Park, Reading, Berkshire RG2 9AX, England

Literary and scientific copyrights belong to ECMWF and are reserved in all countries. This publication is not to be reprinted or translated in whole or in part without the written permission of the Director. Appropriate non-commercial use will normally be granted under the condition that reference is made to ECMWF.

The information within this publication is given in good faith and considered to be true, but ECMWF accepts no liability for error, omission and for loss or damage arising from its use.



Abstract. Satellite instruments specifically designed to monitor atmospheric carbon dioxide concentrations have not been flown to date but high resolution infrared sounders, due for launch in the next few years, may offer the possibility of at least a basic carbon dioxide monitoring capability. This paper explores the sensitivity of this new generation of advanced infrared sounders to changing carbon dioxide concentrations and also compares this with uncertainties due to the atmospheric temperature, water vapour and minor constituent concentrations using the current background errors in numerical weather prediction models as a baseline. The results shown are specifically computed for the Infrared Atmospheric Sounding Interferometer (IASI) which is due to fly on the European METOP platform from 2005. We show that although the carbon dioxide signal is below or at the instrument noise for IASI and that uncertainties in temperature and water vapour errors can dominate, a careful averaging of the retrieved carbon dioxide fields over areas of $500 \times 500 \text{ km}^2$ and 2 weeks should be able to extract changes at the level of 1% or less in the total column carbon dioxide amount.

1. Introduction

The ocean carbon cycle is one of the most complex planetary phenomena. Whilst its main features have been identified, our present knowledge is inadequate either to detect the changes that (almost certainly) have already occurred due to human activities, or to predict the changes (likely to be considerably greater) that can be expected in the future. However in order to recognise human impacts, and assess their significance, we need to address the major areas of uncertainty regarding the functioning of the natural system.

Our current observing system has a significant gap as knowledge of the global carbon cycle is based on sparse sampling on land, at sea and in the atmosphere. For example, we currently reconstruct regional carbon budgets from approximately 100 points. As a consequence, we cannot yet measure the components of the global carbon cycle with sufficient accuracy to balance the budget. Whilst it is known that human activities add 5-6 billion tons (10^9) of carbon each year to the atmosphere, the annual increase in atmospheric CO₂ is equivalent to 3 billion tons of carbon. It had been thought that the oceans absorbed the remainder. However, recent estimates leave at least 1 billion tons unaccounted for. Improvements in the confidence of such estimates, and in our understanding of the uptake mechanisms involved, are therefore urgently needed for reliable predictions of future increases in atmospheric CO₂.

To address these issues, greater geographical and seasonal coverage of CO₂ measurements in the upper ocean and in the atmosphere is required, linked to studies of the relevant physical and biological processes. Satellite measurements of the distribution of global atmospheric CO₂ would in principle fill this gap in scale (Rayner and O'Brien, 2001). Measurements that densely sample the atmosphere would provide a crucial constraint, allowing uncertainty in transport versus other information (on source and sink characteristics) to be separated and reduced. A proof of concept study can already be demonstrated with existing, low spectral resolution instruments (Chedin et. al., 2001) with the NOAA TIROS-N Operational Vertical Sounder (TOVS). Using a set of radiosonde observations collocated with NOAA-10 observations, the measured TOVS radiances have been simulated with an accurate forward radiative calculation and a fixed specification of trace gases. An analysis of the differences between the measured and simulated TOVS brightness temperatures clearly reveals the multi-year trends and seasonal variations of CO₂, CO, N₂O, consistent with the line-by-line calculations of the effect of observed variations in the trace gases. Various proposals have been made for measuring CO₂ from space both using reflected ultra-violet radiation (e.g.

Buchwitz et. al., 2000) and Fourier transform spectrometry (e.g. Park, 1997). Studies are also now being made on the capabilities of the already planned advanced infrared temperature sounders due for launch in the 2002 to 2006 timeframe (Engelen et. al. 2001).

The Infrared Atmospheric Sounding Interferometer (IASI), with its numerous channels and its high spectral resolution, used synergistically with the Advanced Microwave Sounding Unit (AMSU), is one of the potential instrument combinations for monitoring of atmospheric CO₂ concentration from space. This paper describes a sensitivity study applied to simulated IASI data to investigate its capabilities to monitor atmospheric CO₂ concentrations from space (see also Chedin et al., 1999). The natural variability of CO₂ is documented in section 2, the current measurements of CO₂ are described in section 3 and the sensitivity of IASI radiances to CO₂ is presented in section 4. Finally in section 5 the role of ancillary data sources in improving the retrievals of CO₂ is described. The results although computed for IASI are in general applicable to other high resolution infrared sounders which have been launched or are planned in the next decade.

2. The temporal and spatial variability of atmospheric CO₂ concentration

The atmospheric CO₂ concentration is monitored by a network of ground stations of increasing density since the late 1950's. Its space and time characteristics can be described by the superposition of variations at different space and time scales. We will consider all scales, with the exception of the paleo-climatic variability.

At global scales a trend due to anthropogenic inputs of CO₂ to the atmosphere is observed. The concentration increases with time: 1.55 ± 1 ppmv year⁻¹; averaged between 1980 and 1992 (Conway et al., 1994), the extreme values of the annual variation during this period being 0.60 and 2.46 ppmv. Spatially the variations are mainly meridional with a general north-south gradient of about 3.5 ppmv between the north pole (maximum) and the south pole (minimum), this gradient varying from year to year between 3 and 4 ppmv. Large scale spatial variations of small amplitude, about 1 ppmv, are also observed over the ocean in regions of high air-sea exchange.

At shorter time scales a seasonal variation mainly due to the photosynthetic activity of the terrestrial biosphere is observed. Its amplitude is a maximum around 65°N (about 16 ppmv) and decreases to the south. In the southern hemisphere the seasonal variation is of much smaller amplitude and is influenced by the air-sea exchange as well as by the terrestrial biosphere. Figure 1 shows the time evolution of the atmospheric carbon dioxide at different latitudes. A synthesis of these observations with a complete bibliography can be found in Enting and Pearman (1993) and in Bousquet (1997) for more recent results.

At time scales from a few hours to a few days a larger signal is observed. These synoptic variations are due to the meteorological activity which brings to the observing site continental airmasses. For instance when this air comes from industrialised countries they have CO₂ concentrations up to 20 ppmv above the usual concentration in the marine boundary layer as at Mace Head, Ireland (Bousquet et al., 1997). Negative anomalies of the order of 5 ppmv coming from oceanic areas are also observed at this site due to variations of the airmass. Far from continents much weaker synoptic signals are observed. For instance at Amsterdam Island the amplitude of these events coming from South Africa is approximately +/- 1 ppmv (Gaudry et al.,

1990). Such plumes of abnormal CO₂ concentrations simulated by atmospheric transport models are typically 10 degrees wide.

As far as vertical gradients above the ocean are concerned, little is known since only a few aircraft sampling programs have been conducted. Nakazawa et al. (1991) reported the results of an aircraft program between Japan and Australia. Some of their results are summarized in Figure 5 of Enting and Pearman (1993). Recent results from flights above south-east Australia have established a climatology of these vertical profiles up to 8 km (Pack et al., 1996; updated in Pack et al., 1998). In general the variations with altitude are of the order of 1 ppmv but not enough measurements are available at present to be sure this is a globally applicable value.

As far as the isotopic composition is concerned, about 1% of the atmospheric CO₂ is composed of ¹³CO₂. The isotopic composition is usually expressed in δ¹³C where

$$\delta^{13}\text{C meas.} = \left(\frac{(^{13}\text{C}/^{12}\text{C})_{\text{meas.}}}{(^{13}\text{C}/^{12}\text{C})_{\text{ref}}} - 1 \right) * 1000$$

where δ¹³C is expressed in ‰. The reference ratio is : (¹³C/¹²C)_{ref} = 0.0112372.

The isotopic ratio gives indications of the influence of the terrestrial biosphere since photosynthesis and respiration provide an isotopic fractionation. Its seasonal cycle, mainly observed in the northern hemisphere, has an amplitude of about 1‰ and is out of phase with the CO₂ concentration seasonal cycle. The north-south gradient is about 0.2‰, δ¹³C having a minimum at northern latitudes (Trolier et al., 1996). A general trend due to the fossil fuel input to the atmosphere is observed, δ¹³C decreasing by 0.02 ‰ year⁻¹. The measurement accuracy is 0.03‰ (Keeling et al., 1989a and 1989b; Francey et al., 1990; Trolier et al., 1996).

These measurements of atmospheric CO₂ concentration and isotopic composition are used together with atmospheric transport models to identify and quantify sources and sinks of CO₂ to the atmosphere. Several models have been developed. A two dimensional (latitude/height) model has been used by Tans et al. (1990) and Ciais et al. (1995). M. Heimann developed a three dimensional transport model which is widely used, at various spatial resolutions (Heimann and Keeling, 1989; Heimann, 1995). Inverse models are used to quantify CO₂ sources and sinks (Bousquet et al., 1999; Rayner et al., 1999). The horizontal resolution of these models varies between 10° x 10° and 1° x 1° (see Bousquet et al., 1997 for a more complete description).

Thus satellite measurements could be used by such models to study sources and sinks at a global scale, as an interpolation between ground stations. The ground measurements could provide an absolute calibration, the satellite data giving the space and time gradients. In a preliminary test, Rayner and O'Brien (2001) using the method of synthesis inversion estimated that a satellite measuring monthly the column integrated CO₂ concentration over the ocean at 8°x10° resolution would need a precision better than 2.5 ppmv (1.5 ppmv over the ocean) to constrain the inversion better than the surface network. Peylin et. al. (2001) state a requirement of better than 1% of the mean mixing ratio (3-4 ppmv) for an area of 7.5° (longitude) x 7.2° (latitude). For the purposes of this paper we assume a measurement accuracy of 1% of the mean mixing

ratio of CO₂ for a 500 × 500 km² area averaged over 15 days would be of use to the CO₂ monitoring community.

Atmospheric transport models are also used to interpret synoptic variations. They are used to trace back the trajectories of the air masses arriving at the observing station (Ramonet, 1994; Engardt et al., 1996) and determine their origin. Satellite measurements with an accuracy of 10 to 15 ppmv at a resolution of 7.5° and less than one day should allow these plumes to be observed directly. A simulation with a transport model would help to refine this estimate and would give indications of the vertical structure.

3. Review of existing measurements

3.1 Atmospheric PCO₂ measurements

These measurements are either made continuously (sampling rate ~1min) or by taking air samples in flasks which are later analyzed in the laboratory (sampling every one or two weeks). The gas concentration in dry air is measured either by infrared spectrometry or by gas chromatography. The isotopic composition is measured by mass spectrometry. Most stations are in the marine boundary layer, a few of them however are close to or within the continental land masses. For large scale studies using atmospheric transport models, the data from the marine sites are sorted depending on the wind direction in order to discard air masses of local origin or very polluted and to keep only measurements of air masses representative of large oceanic areas. The CO₂ concentration measurements of the ground stations have been inter-calibrated and the accuracy is usually about 0.1 ppmv for monthly means, some stations being biased by a few tenths of ppmv (about 0.3). The flask samples are always taken in pairs and if the two flasks differ by more than 0.4 ppmv, the measurement is eliminated. The ¹³C measurements are not intercalibrated, but this is now underway. The best accuracy is 0.03‰ (Keeling et al., 1989a; Francey et al., 1990; Trolier et al., 1996).

Since Keeling (1960) started the first monitoring station in 1958 at Mauna Loa (Hawaiï), a network has evolved to more than 120 stations. They are far from being evenly distributed, the network being much denser in the northern hemisphere. The ground stations are complemented by programs of repeated measurements along ship tracks (Pacific Ocean, Southern Ocean) and onboard aircraft to get vertical profiles.

The measurements, including paleo-measurements obtained from ice cores, are accessible in the data base of the Carbon Dioxide Information Center (CDIAC). The existing data have been analyzed and extended to provide an homogeneous database intended for modellers using atmospheric transport models to constrain sources and sinks of CO₂ at a global scale. These extended data are accessible on the GLOBALVIEW database (GLOBALVIEW- CO₂ 2000). Details of the measuring techniques and the extension method can be found in Masarie and Tans (1995) and in references therein. As far as the CO₂ concentration in sea water is concerned it is generally measured onboard ships. The first results from autonomous drifting buoys are being published (Hood et al., 1999 ; Hood and Merlivat, 2001). Many data sets are accessible in the CDIAC.

3.2 Satellite wind speeds

Satellite wind speed data are available from 1985. As the wind direction is not used to determine the air-sea CO₂ flux all microwave instruments can be used : altimeters, microwave radiometers and scatterometers. The accuracy of the various instruments has been extensively studied (see Boutin and Etcheto, 1991; Boutin et al., 1996 and references therein). It depends on the instrument, about 1.3 m s⁻¹ for comparisons with in-situ buoy data. When weekly gridded satellite fields from two instruments are compared it can decrease to 0.9 m s⁻¹. Table 1 summarises the instruments that have been used to monitor the air-sea CO₂ exchange coefficient.

Satellite Name	Sensor type	Starting date	End date	Remark
Geosat	Altimeter	March 1985	April 1989	
SSM/I	Microwave radiometer	July 1987	continued	DMSP series
ERS-1	Scatterometer & altimeter	July 1991	May 1996	
Topex/Poseidon	Altimeter	October 1992	continued	
ERS-2	Scatterometer & altimeter	April 1995	Jan 2001	May resume
NSCAT	Scatterometer	Sept 1996	June 1997	
QuikScat	Scatterometer	June 1999	continued	

Table 1 Recent satellite wind sensors

The air-sea CO₂ flux at local and short time scales can be parametrized by:

$$\text{Flux} = K \Delta\text{PCO}_2$$

where K is the exchange coefficient and ΔPCO_2 the air-sea CO₂ partial pressure gradient. The exchange coefficient which is dependent on the turbulence in the sea surface microlayer can be parametrized as a function of the wind speed at the ocean surface. The parametrization also takes into account a weaker dependence on the sea surface temperature. The exchange coefficient is influenced to a lesser extent by other parameters but no parametrization exists at present for these phenomena. The two most commonly used parametrizations are given by Liss and Merlivat (1986) and Wanninkhof (1992). The dependence of K on wind speed is non-linear so that averaged wind speed, such as provided by meteorological models, are unsuitable to derive K (Boutin and Etcheto, 1991) but instantaneous satellite wind speed measurements can be used. A long term monitoring has been performed using several instruments flying at different times (Etcheto et al., 1991; Boutin and Etcheto, 1997). The continuity should be ensured in the future with the launch of several new scatterometers: SEAWINDS on board ADEOS-2 and ASCAT on board METOP.

3.3 High resolution infrared atmospheric sounders

Fourier transform spectrometers have been launched into space to record atmospheric spectra using either a limb-viewing geometry for stratospheric and upper tropospheric soundings, or a nadir-viewing mode for remote sensing of the troposphere. New instruments based on this technology will fly on polar-orbiting satellites within the next decade, for numerical weather prediction (NWP), climate and chemical composition studies. The analysis of each atmospheric spectrum provides information on the atmospheric

state (temperature and composition) at the location of the measurement. Important regions of the spectrum measured are the vibrational-rotational CO₂ lines, which provide the atmospheric temperature information.

Some of the current and planned high resolution advanced infrared sounders are listed in Table 2. The Infrared Atmospheric Sounding Interferometer (IASI) is scheduled for launch in 2005 onboard the European METOP-1 platform. It is a high resolution Fourier transform spectrometer designed to record atmospheric spectra using thermal emission from the atmosphere/surface. A precursor of this mission was the Interferometric Monitor for Greenhouse Gases (IMG) instrument (Kobayashi et al., 1999a; 1999b), launched on the Japanese Advanced Earth Observing System (ADEOS) in August 1996. Ten months of data are available, until the satellite stopped operating (June 1997) due to the failure of its solar panels. The Atmospheric InfraRed Sounder, AIRS, will be launched on the NASA Aqua polar orbiting platform (Aumann and Pagano, 1994). The notable difference between AIRS and IASI is that the radiometric noise is much less (~0.1K) for AIRS in the 4.4 micron CO₂ band because of its actively cooled detectors. The Cross-track Interferometric Sounder (CrIS) is scheduled to fly on the NPOESS (National Polar-orbiting Operational Environmental Satellite System) Preparatory Program (NPP) satellite in a similar timeframe to IASI and also on the operational NPOESS satellites themselves at the end of the decade. Unlike IASI it does not sample the entire spectrum but 3 parts as defined in Table 2 and the spectral sampling and resolution for CrIS is lower than for AIRS and IASI.

Parameter	Advanced Sounder			
	IMG	AIRS	IASI	CrIS
Instrument type	Interferometer	Grating Spectrometer	Interferometer	Interferometer
Satellite Agency	NASDA	NASA/JPL	EUMETSAT/CNES	NOAA IPO
Spectral range (cm ⁻¹)	600-3030	649-1135; 1217-1613; 2169-2674	Contiguous 645-2940	650-1095; 1210-1750; 2155-2550
Number of channels	59623	2378	8461	~1300
Unapodised spectral resolving power/spectral sampling (cm ⁻¹)	10000-20000 0.03-0.04 cm ⁻¹	1000-1400 ~ ν /2400	2000-4000 0.25 cm ⁻¹	900-1800 0.625/1.25/2.5 cm ⁻¹
Spatial footprint (km)	8	13.5	12	14
Nominal Altitude (km)	800	705	833	824
Sampling density per 50km ²	1/86 km on track	9	4	9
Power (W)	150	225	200	86
Mass (kg)	115	176	230	81
Platform	ADEOS	Aqua	Metop-1	NPP and NPOESS
Nominal launch date	17 August 1996	2002	2005	2006(NPP), 2009(NPOESS)

Table 2 Summary of advanced sounder instrument characteristics (note the CrIS values are provisional)

The results presented in this paper refer to simulated IASI data and real IMG data. They have different spectral resolutions, and spatial and temporal sampling due to their different objectives, which are climate/chemistry research for IMG and operational NWP for IASI. This results in a trade-off between spectral resolution and horizontal sampling. The IMG spectrometer records atmospheric spectra using an optical path difference (OPD) of 10 cm, which corresponds to an apodized spectral resolution of 0.1 cm⁻¹,

whereas IASI uses an OPD ranging from -2 cm to +2 cm, leading to a spectral resolution of 0.5 cm⁻¹ (apodized). The difference in spectral resolution is illustrated in Figure 2, which shows calculated nadir radiances obtained at each instrumental resolution in the 15µm CO₂ absorption band, as well as a spectrum measured by IMG.

IASI has a field of view, co-incident with AMSU-A, sampled by a matrix of 2x2 circular pixels of 12 km each and will provide measurements with a good horizontal coverage due to its ability to scan across track with a swath width of 1100 km, whereas IMG only provides nadir measurements with a footprint of 8 x 8 km. For technological reasons, the full spectral range covered by these instruments is subdivided in three spectral bands with different radiometric noise associated with the performance of each detector. The latest estimate of the noise for IASI is plotted in Figure 3 from Cayla (2001).

Atmospheric spectra recorded by the IMG have been analysed by different groups either for the retrieval of temperature and water vapor (Amato et al., 1999; Lubrano et al., 2000) or inversion of trace gas concentrations (Clerbaux et al., 1999; Hadji-Lazaro et al., 1999, Turquety et al. 2001). All these papers report the good quality of recorded spectra but highlight the lack of ancillary data required to perform accurate retrievals. A detailed instrumental spectral response function is not available, and cloud contamination information is not provided, but may be derived directly from the radiance spectra (Hadji-Lazaro et al., 2001). To the best of our knowledge, no studies have been reported on direct measurements of CO₂ using these spectra, which would require global scale accurately measured temperatures and surface emissivities. Furthermore, as discussed in Section 2, the maximum CO₂ variability (~16 ppmv at mid-latitudes) is expected between mid-April and end of August. But as the ADEOS platform stopped operating at the end of June, the IMG data is not ideal to observe this maximum amplitude of the variation.

Another interesting possibility is to study the ratio of C¹³O₂ versus C¹²O₂, which, as explained in Section 2, provides an indication of the CO₂ sources and sinks. The high spectral resolution provided by the IMG instrument allows the spectral contribution of C¹²O₂ in the rotational vibrational ν_2 band to be distinguished from other absorbing contributions in hot bands and isotopes. Figure 2 shows the absorption contribution from the different isotopes in the 725-740 cm⁻¹ spectral range, which was found to be the optimal spectral range to study isotopic composition. Although the absorption features are clearly seen, small variations of the isotopic ratio may be difficult to retrieve. These retrievals are obviously not possible with IASI as can be seen in Figure 2.

4. Sensitivity studies for IASI measurements

4.1 Radiative transfer models used for simulations

To investigate the potential for IASI to detect CO₂ changes from top of atmosphere radiance measurements two independent sets of simulations, using different models, were performed to determine how much the radiances are changed by varying the CO₂ concentration by typical amounts. In addition atmospheric temperature, water vapor, ozone and nitrous oxide profiles and surface emissivity and temperature were also varied to gauge their effects on the radiances. The results from both simulations were similar giving confidence in them. Both radiative transfer models are described briefly below.

Firstly the line-by-line atmospheric transmittance and radiance code, GENLN2 (Edwards, 1992), was used with line parameters from the 1996 version of the High-Resolution Transmission (HITRAN) molecular database (Rothman et. al, 1998). Carbon dioxide line coupling was modelled using the line coupling coefficients included (Strow et. al, 1994). Spectra were computed at 0.001 cm⁻¹ resolution and then convolved with the appropriate (Cayla, 1996) IASI Spectral Response Function (ISRF) to obtain the level 1C IASI apodized spectra. The transmittance calculations were made on 43 fixed pressure levels from 0.1 to 1013 hPa. For the radiance stage of the line-by-line computations, the surface temperature was set equal to the 1013 hPa value of the temperature profile and a value of 0.98 was assumed for the surface emissivity. This value is expected to cover a broad range of surface classes for the frequencies of interest in this study (Snyder et. al, 1998). Radiances were simulated for sub-arctic winter, mid-latitude summer, mid-latitude winter and tropical profiles taken from the AFGL set of atmospheric constituent profiles.

To complement the above, similar computations were carried out using the Automatized Atmospheric Absorption Atlas (4A) fast line-by-line transmittance and radiance computation model (Scott and Chedin, 1981). 4A relies on the use of a vast archive (the atlas) of optical depths created, once and for all, using the line-by-line and layer-by-layer model, STRANSAC, (Scott, 1974; Tournier et. al. 1995) in its latest 2000 version with up to date spectroscopy from the GEISA spectral line catalogue (Jacquinet-Husson et. al. 1999). Spectra were computed at a resolution of the order of the smallest line half-width (about 5.10⁻⁴ cm⁻¹) and then convolved with the IASI response function (unapodized). Transmittance computations were made on 40 pressure levels from 1013 hPa to 0.05 hPa. The surface emissivity varied with frequency according to Masuda et. al. (1988) for sea water.

4.2 Sensitivity to changes in CO₂ concentrations

The reference spectra were computed assuming a climatological concentration value for CO₂ equal to 376 ppmv. This is the predicted concentration value for the year 2005 assuming an annual mean CO₂ mixing ratio of 356 ppmv for the year 1992 (Conway et. al, 1994) and a yearly increase rate of 1.5 ppmv (Schimel et al., 1995). For each profile considered in the study, test spectra were computed by perturbing the annual mean CO₂ mixing ratio profile by half the value of the mean peak-to-peak amplitude of the seasonal CO₂ cycle (for GENLN2 only the tropospheric amount was perturbed). This is 9ppmv for mid-latitude and subarctic winter profiles and 4 ppmv for the tropical profile (Conway et. al, 1994). As a result of this, the CO₂ mixing ratios used in the computations were: 380 ppmv for the tropical profile, 385 ppmv for the mid-latitude winter and sub-arctic profiles and 367 ppmv for the mid-latitude summer profile. Figure 3 shows, for the above profiles, the difference in radiance between the reference and perturbed CO₂ case for the frequency range 650 to 850 cm⁻¹ (hereafter referred to as LW) in the upper panel. The radiance difference for all the plots is expressed in terms of the equivalent brightness temperature difference, at a reference blackbody temperature which is the mean scene temperature at each wavelength (i.e. average of all simulated spectra). This can be directly compared with the instrument noise also plotted which is the estimated IASI radiometric noise at the reference temperature (Cayla, 2001).

For the mid-latitude winter and mid-latitude summer profiles the predicted change in radiance is 0.25K just above the noise. Smaller values are observed for the subarctic winter (~ 0.2 K) and tropical profile (~ 0.1 K). Note that the noise curve plotted in Figure 3 is the noise for a single IASI pixel. As the signal is only at the level of detectability an averaging of the IASI retrievals will be necessary for a CO₂ retrieval to be

possible. Another option would be to retrieve CO₂ as part of the routine assimilation process of a NWP model, and then average the daily retrieved CO₂ fields.

Results are also shown for the spectral region 2200 to 2500 cm⁻¹ (hereafter referred to as SW) in Figure 3. In this case the signal (predicted changes in brightness temperature) peaks at +0.3K (for mid-latitude winter profiles) and up to -0.3K (for the mid-latitude summer profile). This is well below the instrument noise at 2250 cm⁻¹ for a single IASI pixel measurement.

In addition to perturbing the entire profile, which is not a change encountered in nature, runs were also made where only the 700-200 hPa layer was perturbed and also the 700hPa-surface was perturbed. The results (not shown) clearly show nearly all the radiance signal comes from changes in CO₂ concentration in the 700-200 hPa layer not the layer close to the surface so that IR sounders will not be suitable for monitoring changes of CO₂ in the atmospheric boundary layer.

4.3 Sensitivity to changes in temperature, humidity and other minor gases

The influence of uncertainties in temperature and humidity on the CO₂ retrieval was quantified by perturbing the mean temperature and humidity profiles by an amount given by the mean error in the background (from a 6 hour forecast) ECMWF model fields for each latitude band. This represents the "background" error assumed in the retrieval/assimilation schemes. These errors in temperature and specific humidity were taken from the 1999 version of the ECMWF 50 level model analysis system. It is likely that future developments in data assimilation, NWP model formulation and increased use of satellite data will reduce these errors so those assumed here are an upper limit. For each of the atmospheres considered in the study a different mean error profile was used. The error varies with level, the typical range being 0.8K at the surface to 3K in the stratosphere for temperature and 2000 to 0.02 ppmv for water vapor mixing ratio. The profiles used in the perturbed cases were obtained by increasing the reference profiles by the mean error profile for that atmosphere. For temperature the results are shown in Figure 4 where for each of the atmospheres the radiance difference between reference and perturbed case is shown. For all atmospheres, perturbing the temperature profile gives a signal greater than that obtained by perturbing the CO₂ profile. For the LW region of the spectrum (upper panel of Fig 4) the uncertainty due to temperature gives a signal three times greater than the CO₂ signal. The SW region (lower panel of Fig. 4) is less sensitive to temperature uncertainties, due to the non-linearity of the Planck function, but still gives a signal about twice that of the CO₂ changes.

The effect of CO₂ anomalies is likely to be a bias, whereas the signal from the perturbed temperature profile in general is expected to be randomly distributed, over a reasonable time period (~2 weeks) and should average out when a large sample of IASI radiances is considered. However there are conditions in some locations where the temperature errors in the model and CO₂ errors may be correlated and this will need to be studied in more detail with in-situ data.

The sensitivity of the radiances to the perturbation of the humidity profile is shown in Figure 5. As for the temperature sensitivity, the signal resulting from the perturbation of the humidity profile can be several times greater than the signal from the CO₂ variation. However it is worth noting that several "window" regions can be identified (e.g. 721cm⁻¹ for the LW and beyond 2245 cm⁻¹ for the SW) where the effect of

water vapor is negligible or absent in this part of the spectrum. This suggests the parts of the spectrum which are not sensitive to water vapor should be used for the CO₂ retrieval.

For the sensitivity to uncertainty in ozone concentrations Figure 6 shows the radiance response for a mid-latitude summer atmosphere (474 Dobson units) when the ozone amount is reduced by 13.5% which is a typical magnitude of the variability in ozone at mid-latitudes. In the LW region the peak radiance perturbation is -0.7K close to 725 cm^{-1} but there is a window at 720 cm^{-1} . In the SW the sensitivity to ozone becomes negligible above 2240 cm^{-1} .

The sensitivity to nitrous oxide, N₂O, was checked by comparing the mean of the US standard atmospheres N₂O concentration with the tropical profile. The results are shown in the lower panel of Figure 6. There are no significant absorption bands due to N₂O below 1100 cm^{-1} so the LW region is unaffected. In the SW region there is a sensitivity which reduces to zero at 2255 cm^{-1} . No sensitivity to methane was found in these spectral regions. Carbon monoxide does absorb from $2150\text{-}2200\text{ cm}^{-1}$ in the same region as N₂O.

In summary for the LW part of the spectrum temperature, water vapor and ozone all affect the same region of the spectrum as CO₂, making the choice of channels in this LW region not affected by either water vapor or ozone more difficult. In the SW only temperature affects the same region of the spectrum as CO₂ and to a lesser extent than in the LW. Hence although the sensitivity to CO₂ is less relative to the IASI noise in the SW there is less interference from other absorbing molecules there.

4.4 Sensitivity to changes in surface temperature and land surface emissivity

This test was carried out only for the sub-arctic atmosphere as with low water vapor amounts this will give an upper bound to the sensitivity of the surface emissivity. The perturbed surface temperature was set equal to the reference value plus 1 K whereas the perturbed land surface emissivity was set equal to 0.97 a change of 0.01. Results are shown in Figure 7. For the $645\text{ to }710\text{ cm}^{-1}$ wavenumber region the radiance is not sensitive to changes in emissivity whereas in the $710\text{ to }745\text{ cm}^{-1}$ region the signal is still less than the CO₂ signal. The signal can be as great as $+0.6\text{ K}$. For the surface temperature case the radiance change is greater than the CO₂ signal for wavenumbers greater than 720 cm^{-1} . In contrast, for smaller wavenumbers the signal coming from the surface temperature perturbation is either zero or slightly less than the CO₂ signal. Elsewhere the signal peaks at -1K for the window regions. For the SW region the sensitivity to surface parameters becomes negligible at frequencies between $2250\text{ and }2380\text{ cm}^{-1}$. Over water the uncertainty in emissivity and temperature is much less making CO₂ retrievals over the ocean easier.

4.5 Impact of errors in spectroscopic databases

Persistent discrepancies are still observed between line-by-line-simulated and observed high resolution spectra, both in some CO₂ and H₂O absorption bands. These errors are mostly due to the inaccuracies in the line intensities presently used and for CO₂ in the line mixing formulation. Difficulties also exist for measuring accurate in-situ atmospheric water vapor amounts to validate the spectroscopic parameters. These problems do not affect the conclusions on the relative amplitude of the signal due to CO₂ perturbations reported here. However, such limitations should be taken into account when selecting the best set of channels for monitoring CO₂.

4.6 Signal to noise and averaging

The above results have illustrated the sensitivity of IASI to CO₂ perturbations. This section deals with the averaging required to obtain CO₂ profiles that differ significantly from the mean background field. Figure 8 shows the ratio of the IASI response to CO₂ perturbations to the IASI nominal noise, computed at the temperature “seen” by each channel (function of frequency), for the 4 atmospheric situations considered (tropical : perturbation of 4 ppmv ; mid-latitude winter and summer and sub-arctic winter : perturbation of 9 ppmv). A signal to noise of unity is reached for channels between 704 cm⁻¹ and 745 cm⁻¹ but for channels at 2250 cm⁻¹ only values of 0.4 are reached for the mid-latitude summer profile perturbation and a single measurement. Significant averaging is therefore required to raise the CO₂ signal to noise ratio. Figure 9 gives the number of IASI pixels to be averaged in order to get a signal to noise ratio of 1, as a function of the wavenumber. In the 700 to 750 cm⁻¹ region only 1-2 IASI observations are typically required to raise the signal above the noise whereas at 2250 cm⁻¹ at least 10 observations are required.

Over a 500 × 500 km² area there will be ~12,000 IASI measurements over a 15 day period of which ~25% would be expected to be insignificantly contaminated by cloud giving 3000 useful measurements. This translates to a signal to noise ratio of >30 for the LW channels and >5 for the SW channels for a 1% change (3.8 ppmv) in total column CO₂ over 15 days. This is broadly consistent with the requirements for monitoring the atmospheric CO₂ concentration from space (see Section 2).

However, to be successful, consideration must also be given to selecting channels to minimise the ‘interference’ from other atmospheric and surface variables. Channels not sensitive to surface characteristics are quite easy to select but channels not sensitive to water vapor and other minor gases are more difficult, but feasible, to identify. Signals coming from the temperature errors cannot be avoided but, as pointed out in section 4.3, the signal from CO₂ is likely to be a bias whereas the signal from errors in temperature is expected to be randomly distributed over a reasonable time period (~15 days). These constraints are compatible with studies at a global scale of the atmospheric CO₂ sources and sinks provided a 15 day mean accuracy approaching 1% of the total column amount can be obtained, which is a challenging but not impossible target for IASI measurements.

5. Evaluation of the role of ancillary data

5.1 Independent imagers for cloud detection and SST retrieval

One of the principal disadvantages of infrared sounders is that they are strongly affected by any cloud in the field of view. In order to ensure the radiances used for inferring CO₂ amounts are not contaminated by cloud, and hence give an erroneous retrieval, a higher resolution imager is useful to ensure all significant clouds can be detected. The Advanced Very High Resolution Radiometer (AVHRR) which has 1km fields of view will be on the same platform as IASI and can be used for cloud detection. It has visible channels and so during the day reflected sunlight can be used to discriminate between low clouds and sea surface. Another advantage of these imaging radiometers is the radiometric noise is less than for IASI (e.g. 0.1K for AVHRR vs 0.25K for IASI) allowing a less noisy radiance field for cloud detection.

In addition, for the IASI channels, which are sensitive to the surface, it is important to have an accurate estimate of the sea or land surface temperature as shown in the previous section in order to have confidence in the retrieved CO₂ amounts from IASI. Accurate measurements of sea surface skin temperature (SSST) can be made using the IASI window channels in a range of different wavelengths in cloudfree areas. However there are problems with using the IASI window channels to infer SSST as the 10km field of view means cloudfree scenes over some parts of the ocean are rare. Imaging radiometers such as AVHRR are more likely to “see” between the gaps in the clouds. This improved capability for cloud detection and coverage of cloudfree areas should improve the accuracy of the SSSTs and hence the CO₂ retrievals.

5.2 Synergy of AMSU and IASI

In order to be confident any change in CO₂ concentrations from IASI are not just a consistent change in atmospheric temperature over the region of interest an independent measurement of atmospheric temperature must be made at the same time as the IASI retrieval. This is possible with the AMSU-A radiometer on METOP, which sounds the atmospheric temperature using the 50-55 GHz oxygen absorption band in contrast to the CO₂ bands traditionally, employed in the infrared. Any changes in CO₂ concentration will not affect temperature profiles retrieved using the microwave oxygen absorption band.

To determine exactly how sensitive the AMSU-A channels are to the temperature profile a radiative transfer model for the AMSU channels (RTTOV-5 as described in Saunders et. al, 1999) was used to compute top of atmosphere AMSU-A brightness temperatures for the same standard atmospheres used in section 4. The computation was carried out for the standard profile and then the whole profile was incremented by a constant value at all levels and a revised brightness temperature computed. The temperature increments applied to the profiles corresponded roughly to the change in temperature for each profile that was equivalent to the change in radiance seen in the IASI spectra for a seasonal change in CO₂. For example as Figure 10 shows for a mid-latitude winter atmosphere the change in radiance due to CO₂ is about 0.2K and so this was the value by which the midlatitude winter profile was incremented for the AMSU-A calculations. The results for three latitude bands are shown in Figure 10 for AMSU channels 1-12 (the remainder do not sound the tropospheric temperature profile). A realistic sea surface emissivity for tropical and mid-latitude winter profiles was assumed and constant value of 0.9 (for snow) for the arctic profile was used which explains the different responses in the AMSU-A window channels (1-3). The response for the mid-latitude and arctic profiles is twice that of the tropical profile (because of the larger seasonal variation in CO₂ at high latitudes) but in all cases is less than the specified instrument radiometric noise for each channel for a single radiance measurement. It is worth noting that the actual noise values for AMSU-A on NOAA-15 measured in the laboratory before launch were in many cases less than the specified values plotted but they will be different for each instrument.

Averaging the temperature field reduces the errors allowing a mean temperature change signal to be extracted. It is important to bear in mind however that when studying temporal trends in the AMSU-A or IASI data the assumption does have to be made that there are no drifts in absolute calibration between both instruments. Regular collocations with radiosondes and aircraft reports can help to quantify drifts to within 0.1K. Collocations with other satellite instruments (e.g. HIRS on METOP, AIRS on AQUA, IASI on another METOP etc) will also be valuable for quantifying drifts. The experience of the MSU and AMSU-A radiometers suggests the microwave radiometers once launched are very stable in terms of radiometric



calibration. Infrared radiometers or interferometers are more prone to contamination of the optics and a subsequent change of sensitivity with time although to first order this drift should be accounted for with the on-board calibration.

In summary the AMSU-A channels can be used as a constraint on the temperature assumed in the IASI CO₂ retrieval probably to a level of 0.1K. This should allow changes in CO₂ concentration of about 1% to be confidently inferred from the IASI radiances using the AMSU to define the temperature profile. Similarly the Microwave Humidity Sounder (MHS) can also provide an independent measurement of the humidity profile using the 183 GHz water vapor absorption line. This is less critical as channels can be selected from the IASI spectrum which are insensitive to the water vapor concentration.

5.3 GPS radio-occultations

Another source of independent temperature measurements is the radio-occultation GPS (Global Positioning System) soundings which are planned from METOP and other satellites. The advent of the GPS allows receivers placed on low Earth orbiting spacecraft to view the GPS satellite constellation through atmospheric limb paths and enables the refractive index profile of the atmosphere to be retrieved. The refractive index data can then be related to the temperature and humidity profile (Healy and Eyre, 2000). The concept of combining this information with interferometer radiances for climate monitoring is discussed by Goody et al (1998). These data either used in the vicinity of a IASI measurement or assimilated in a NWP model to improve the model temperature and humidity fields should be a useful additional data source to help remove uncertainties in the temperature and water vapor fields. These measurements are not subject to drifts due to calibration in contrast to radiometer measurements.

6. Conclusions

Monitoring atmospheric CO₂ concentrations from currently planned advanced IR sounder observations is clearly a challenging problem and will need careful pre-processing of the radiances in order not to swamp the CO₂ signal with other effects (e.g. undetected cloud, errors in assumed temperature profile). For a CO₂ retrieval to be possible the radiances must not only be *sensitive* to CO₂ concentration changes but also *separable* from other factors that influence them. IASI channels sensitive to the CO₂ perturbation but only weakly sensitive to uncertainties in water vapor, ozone, minor constituents and surface characteristics can be identified in both the SW and LW parts of the infrared spectrum. For the 15 micron CO₂ band uncertainties in temperature, water vapor and ozone all affect the same region of the spectrum as CO₂ making the choice of channels in this wavelength region not affected by either water vapor or ozone more difficult. In the 4.4 micron band only temperature affects the same region of the spectrum as CO₂ and to a lesser extent than at 15 micron. However the instrument noise for IASI is much higher relative to the signal at the shorter wavelengths. Therefore there is a trade-off between sensitivity to CO₂ relative to the instrument noise and reducing the interference from other absorbing molecules. The SW and LW parts of the spectrum should be used simultaneously to optimize the CO₂ retrieval. For IASI the uncertainties in the atmospheric temperature and humidity profile can be reduced by including the coincident AMSU-A and MHS sounder data in the assimilation or retrieval process. It is worth noting that AIRS has a much lower instrument noise than IASI in the SW band and as a result may offer a better capability for monitoring CO₂ despite its lower spectral resolution.

Based on current IASI noise estimates the simulations suggest an averaging of retrieved CO₂ fields of 500 × 500 km² in space and 15 days in time to achieve an accuracy of less than 1% in total column CO₂ amount. The CO₂ concentration information is primarily in a deep layer from the middle to upper troposphere. This should allow a global scale study of atmospheric CO₂ sources and sinks as long as the changes are not confined to the boundary layer. Ground measurements could provide absolute calibration, the satellite data giving the space and time gradients. Synoptic scale variations are more difficult since the required temporal resolution should be less than one day and although in this case the required accuracy is only 10 to 15 ppmv, the uncertainties in atmospheric temperature cannot be distinguished from the CO₂ changes.

The optimal approach to infer the 3 dimensional global distribution of CO₂ from these sounders is to use a variational data assimilation system (e.g. 4D-Var as described in Klinker et. al., 2000) which includes CO₂ as a variable in the model atmospheric state vector. The model background fields of temperature, water vapour and other minor constituents, including CO₂, are provided from a short range forecast from an analysis of the initial atmospheric state. This analysis has simultaneously assimilated all the observations available both direct (e.g. radiosonde profiles, aircraft reports) and indirect (e.g. radiances) to define the 3 dimensional state of the atmosphere at a given time. This assimilation process results in a reasonably accurate estimate of the initial atmospheric state compared with say a first guess climatological profile. Selected channels of the advanced sounder radiances, away from interfering species, would be assimilated along with all the other observations, taking into account their respective errors, using a fast radiative transfer model and its gradient as described by Engelen et. al. (2001). Forecast error covariances for carbon dioxide concentration will need to be estimated in order to distribute the inferred CO₂ perturbations to where the concentrations have their largest uncertainties in the model space. Care will need to be taken to estimate these errors as they strongly influence the analysed CO₂ fields. The microwave sounder radiances and GPS measurements will be assimilated simultaneously with the infrared radiances to help constrain the temperature and humidity profiles.

Alternatively stand-alone retrievals of CO₂ concentration and temperature profiles based on for example non-linear neural networks trained on a diverse CO₂ profile dataset could also be developed to provide an NWP independent dataset for climate studies. This has been done with Microwave Sounding Unit radiances to infer a climate record of the lower stratospheric mean temperature (Spencer and Christy, 1993).

Finally clear sky IMG spectra, collocated with accurate temperature and moisture profiles, surface temperatures and emissivities have been processed to show their capability to study the ratio of ¹³CO₂ to ¹²CO₂, which could provide an indication of the nature of the CO₂ sources and sinks. Unfortunately this capability is beyond the limits of the advanced IR instruments now planned for launch on operational meteorological platforms.

Future work to better assess how advanced infrared sounder data can provide information on CO₂ concentration should include the following:

- An assessment of whether our current knowledge of the spectroscopic parameters (e.g. line strengths, widths, coupling coefficients) is adequate for all CO₂ isotopes and to identify regions of the spectrum where the spectroscopy is well understood and documented.



- determine the number of pixels to be averaged in space and time as a function of the required CO₂ accuracy and more accurate estimates of instrument noise.
- create a dataset of CO₂ concentration profiles representative of natural and human-induced variability
- upgrade fast radiative transfer models (e.g.. RTIASI, Matricardi and Saunders (1999) or the neural network model, Advanced Rapid Radiance Reconstruction Network (A3R-N) by Montandon et. al. (2001)) to include CO₂ as a variable gas and to compute the Jacobians with respect to CO₂.
- Undertake an information content study (e.g. Rodgers, 1976) to determine how separable the CO₂ signal is for IASI radiances and IASI + AMSU radiances. The optimal IASI channels for CO₂ concentration retrievals can also be determined from this study.

Acknowledgements

This work was carried out under a EUMETSAT funded contract (98/310). F. Cayla provided the latest IASI noise figures for the calculations presented here. We thank P. Ciais for helpful discussions. The IMG level 1c data was provided by IMGDIS/ERSDAC for which the authors are grateful.

References

- Amato, U., V. Cuomo, I. De Feis, F. Romano, C. Serio and H. Kobayashi, 1999: Inverting for geophysical parameters from IMG radiances. *IEEE Trans. Geosci. and Remote Sens.*, **37**, 1620-1632.
- Aumann, H.H. and R.J. Pagano, 1994: Atmospheric infrared sounder on Earth observing system. *Optical Eng.*, **33**, 776-784.
- Bousquet, P., 1997: Optimisation des flux nets de CO₂: assimilation des mesures atmosphériques en CO₂ et en ¹³CO₂ dans un modèle de transport tridimensionnel, Thèse Paris 6.
- Bousquet, P., A. Gaudry, P. Ciais, V. Kazan, P. Monfray, P.G. Simmons, S.G. Jennings and T.C. O'Connors, 1997: Atmospheric CO₂ concentration variations recorded at Mace Head, Ireland, from 1992 to 1994. *Phys. Chem. Earth*, **21**, 477-481.
- Bousquet, P., P. Peylin, P. Ciais, M. Ramonet and P.: Monfray, 1999: Inverse modelling of annual atmospheric CO₂ sources and sinks. 1. Method and control inversion. *J. Geophys. Res.*, **104**, 26161-26178.
- Boutin, J. and J. Etcheto, 1991: Intrinsic error on the air-sea CO₂ exchange coefficient resulting from the use of satellite wind speeds. *Tellus*, **43B**, 236-246.
- Boutin, J., L. Siefert, J. Etcheto, and B. Barnier, 1996: Comparison of ECMWF and satellite wind speed from 1985 to 1992. *Int. J. Remote Sens.*, **17**, 2897-2913.
- Boutin, J., and J. Etcheto, 1997: Long term variability of the air-sea CO₂ exchange coefficient: Consequences for the CO₂ fluxes in the equatorial Pacific Ocean. *Global Biogeochem. Cycles*, **11**, 453-470.
- Buchwitz, M.V., V. Rozanov and J.P. Burrows, 2000: A near infrared optimized DOAS method for the fast retrieval of atmospheric CH₄, CO, CO₂, H₂O and N₂O total column amounts from Schiamachy ENVISAT-1 nadir radiances. *J. Geophys. Res.*, **105** (D12), 15231.

- Cayla, F., 1996: Simulation of IASI spectra. *CNES document IA-TN-0000-5627-CNE* (Centre National d'Etudes Spatiales, Toulouse).
- Cayla, F., 2001: Personal communication.
- CDIAC: Carbon Dioxide Information Analysis Center, web site <http://cdiac.esd.ornl.gov/cdiac>.
- Ciais, P., P.P. Tans, M. Trolier, J.W. White and R. Francey, 1995: A large northern hemisphere terrestrial CO₂ sink indicated by the ¹³C/¹²C ratio of atmospheric CO₂. *Science*, **269**, 1098-1102.
- Chedin, A., N.A.Scott, R. Saunders, M. Matricardi, J. Etcheto and C. Clerbaux, 1999: IASI capability to monitor CO₂. *Final Report, EUMETSAT Contract N° 98/310*.
- Chedin, A., S. Serrar, R. Armante and N.A. Scott, 2001: Signatures of annual and seasonal variations of CO₂ and other greenhouse gases from comparisons between NOAA/TOVS observations and model simulations. Accepted by *J. Climate*.
- Clerbaux, C., J. Hadji-Lazaro, S. Payan, C. Camy-Peyret, and G. Mégie, 1999: Retrieval of CO columns from IMG/ADEOS spectra.. *IEEE Trans. Geosci. Remote Sens.*, **37**, 1657-1662.
- Conway, T.J., P.P. Tans, L.S. Waterman, K.W. Thoning, D.R. Kitzis, K. A. Masarie and N. Zhang, 1994: Evidence for interannual variability of the carbon cycle from the National Oceanic and Atmospheric Administration/Climate Monitoring and Diagnostic Laboratory Global Air Sampling. *J. Geophys. Res.*, **99**, 22831-22855.
- Edwards, D.P., 1992: GENLN2. A general line-by-line atmospheric transmittance and radiance model. *NCAR Technical note NCAR/TN-367+STR* (National Center for Atmospheric Research, Boulder, Co.).
- Engardt, M., K. Holmen and J. Heintzenberg, 1996: Short-term variations in atmospheric CO₂ at Ny-Alesund, Spitsbergen during spring and summer. *Tellus*, **48B**, 33-43, 1996.
- Engelen R.J., A. Scott Denning, H.R. Gurney and G.L. Stephens, 2001: Global Observations of the carbon budget: I. Expected satellite capabilities for emission spectroscopy in the EOS and NPOESS eras. *J. Geophys. Res.*, (in press).
- Enting, I. G., and G. I. , Pierman, 1993: Average global distribution of CO₂, in *The global carbon cycle*, Ed. M. Heimann, NATO ASI Series, Springer Verlag, 31-64.
- Etcheto, J., J. Boutin and L. Merlivat, 1991: Seasonal variation of the CO₂ exchange coefficient on the global ocean using satellite wind speed measurements, *Tellus*, **43B**, 247-255.
- Francey R.J., F. J. Robbins, C.E. Allison and N.G. Richards, 1990: The CSIRO global survey of CO₂ stable isotopes, *Baseline 1988*, ed. W.S.R., Australia.
- Gaudry, A., P. Monfray, G. Polian and G. Lambert, 1990: Radar-calibrated emissions of CO₂ from South Africa. *Tellus* , **42B**, 9-19.
- GLOBALVIEW-CO2, 2000: Cooperative Atmospheric Data Integration Project - Carbon Dioxide. CD-ROM, NOAA CMDL, Boulder, Colorado [Also available on Internet via anonymous FTP to <ftp.cmdl.noaa.gov>, Path: <ccg/co2/GLOBALVIEW>].
- Goody, R., J. Anderson and G. North, 1998: Testing climate models : an approach. *Bull. Amer. Meteor. Soc.*, **79**, 2541-2549.
- Hadji-Lazaro, J., C. Clerbaux, and S. Thiria, 1999: An inversion algorithm using neural networks to retrieve atmospheric CO concentrations from high-resolution nadir radiances. *J. Geophys. Res.* **104**, 23,841-23,854.



- Hadji-Lazaro, J., C. Clerbaux, P. Couvert, P. Chazette, and C. Boone, 2001: Cloud filter for CO retrieval from IMG infrared spectra using ECMWF temperatures and POLDER cloud data. *Geophys. Res. Lett.*, **28**, 2397.
- Healy S.B. and J. R. Eyre, 2000: Retrieving temperature, water vapour and surface pressure information from refractive-index profiles derived by radio occultation: A simulation study. *Quart. J. Roy. Meteorol. Soc.*, **126**, 1661.
- Heimann M. and C.D. Keeling, 1989: A three-dimensional model of atmospheric CO₂ transport based on observed winds : 2. Model description and simulated tracer experiments, aspects of climate variability in the Pacific and Western Americas, *Geophysical monograph 55*, ed. D. H. Peterson, American Geophysical Union, Washington (USA), 237-275.
- Heimann, M., 1995: The Global Atmospheric Tracer Model TM2. *Rapport n°10*, Max-Planck Institute fur Meteorologie, Hamburg.
- Hood E.M., Merlivat L. and Johannessen T., 1999: Variations of fCO₂ and air-sea flux of CO₂ in the Greenland Sea gyre using high-frequency time-series data from CARIOCA drift-buoys. *J. Geophys. Res.*, **104**, 20571-20583.
- Hood E.M. and L. Merlivat, 2001: Annual to interannual variations of fCO₂ in the northwestern Mediterranean sea : results from hourly measurements made by CARIOCA buoys, 1995-1997. *J. Mar. Res.*, **59**, 113-131.
- Jacquinet-Husson, N., et al., 1999: The 1997 spectroscopic GEISA data bank. *J. Quant. Spectrosc. Radiat. Transfer*, **62**, 205-254.
- Keeling, C. D., 1960: The concentration and isotopic abundances of carbon dioxide in the atmosphere. *Tellus*, **12**, 200-203.
- Keeling C.D., R.B. Bacastow, A.F. Carter, S.C Piper, T.P. Whorf, M. Heimann, W.G. Mook and H.A. Roeloffzen, 1989a: A three-dimensional model of atmospheric CO₂ transport based on observed winds : 1. Analysis of observational data, aspects of climate variability in the Pacific and Western Americas. *Geophysical monograph 55*, ed. D. H. Peterson, American Geophysical Union, Washington (USA), 165-236.
- Keeling C.D., S.C. Piper and M. Heimann, 1989b: A three-dimensional model of atmospheric CO₂ transport based on observed winds : 4. Mean annual gradients and interannual variations, aspects of climate variability in the Pacific and Western Americas. *Geophysical monograph 55*, ed. D.H. Peterson, American Geophysical Union, Washington (USA).
- Klinker, E., F. Rabier, G. Kelly and J.-F. Mahfouf, 2000: The ECMWF operational implementation of four-dimensional variational assimilation. III: Experimental results and diagnostics with operational configuration. *Quart J. Roy. Meteorol. Soc.*, **126**, 1191-1200.
- Kobayashi, H., A. Shimota, K. Kondo, E. Okumura Y. Kameda, H. Shimoda, and T. Ogawa, 1999a: Development and evaluation of the interferometric monitor for greenhouse gases: A high-throughput Fourier-transform infrared radiometer for nadir Earth observations. *Appl. Opt.*, **38**, 6801-6807.
- Kobayashi, H., A. Shimota, C. Yoshigahara, I. Yoshida, Y. Uehara, and K. Kondo, 1999b: Satellite-borne high-resolution FTIR for lower atmosphere sounding and its evaluation. *IEEE Trans. Geosci. and Remote Sens.*, **37**, 1496-1507.
- Liss, P.S., and L. Merlivat, 1986: Air-sea gas exchange rates : introduction and synthesis. In *The Role of Air-Sea Exchange in Geochemical Cycling*, edited by P. Buat-Minard, D. Reidel, Norwell, Mass., pp. 113-127.
- Lubrano, A. M., C. Serio, S. A. Clough, H. Kobayashi, 2000: Simultaneous inversion for temperature and water vapor from IMG radiances. *Geophys. Res. Lett.*, **27**, 2533-2536.
- Montandon, V.A., A. Chedin, P. Aires, R. Armante and N.A. Scott, 2001: The Advanced Rapid Radiance Reconstruction Network (A3R-N) model for IASI radiance simulations (in preparation).

- Masuda, K., T. Takashima and T. Takayama, 1988: Emissivity of pure sea waters for the model sea surface in the infrared window regions. *Remote Sensing of Environment*, **24**, 313-329.
- Masarie, K.A. and P.P. Tans, 1995: Extension and integration of atmospheric carbon dioxide data into a globally consistent measurement record. *J. Geophys. Res.*, **100**, 11593-11610.
- Matricardi, M. and R.W. Saunders, 1999: A fast radiative transfer model for simulation of IASI radiances. *Applied Optics*, **38**, 5679-5691,
- Nakazawa, T. K. Miyashita, S. Aoki and M. Tanaka, 1991: Temporal and spatial variations of upper tropospheric and lower stratospheric carbon dioxide. *Tellus*, **43B**, 106-117.
- Pak, B.C., R.L. Langfelds, R.J. Francey, L.P. Steele and I. Simmonds, 1996: A climatology of trace gases from the Cape Grim over-flights, 1992-1995. In: *Baseline Atmospheric Program Australia, 1994-1995*, Ed. R. J. Francey, A. L. Dick, and N. Derek (editors). Bureau of Meteorology and CSIRO Division of Atmospheric Research. Melbourne, 41-52.
- Pak, B. C., M., Ramonet, P., Monfray, R. J., Francey, and I., Simmonds, 1998: Assessment of the spatial and temporal representativeness of the Cape Gim overflight CO₂ data. In: *Baseline Atmospheric Program Australia, 1996*. Bureau of Meteorology and CSIRO, Division of Atmospheric Research. Melbourne.
- Park, J.H., 1997: Atmospheric CO₂ monitoring from space. *Applied Optics*, **36**, 2701-2712.
- Peylin, P., B. Picard, P. Bousquet, F.M. Breon and P. Ciais, 2001: Potential of column integrated CO₂ fluxes using inverse methods. *4th GEWEX Symposium*, Paris, 10-14 Sept 2001.
- Ramonet, M., 1994: Variabilité du CO₂ atmosphérique en régions australes: comparaison modèle/mesures, *Thèse Paris 6*.
- Rayner, P.J., I.G. Enting, R.J. Francey and R.L. Langenfelds, 1999: Reconstructing the recent carbon cycle from atmospheric CO₂, $\delta^{13}\text{C}$ and O₂/N₂ observations, *Tellus*, **51B**, 213-232.
- Rayner, P.J. and D.M. O'Brien, 2001: The utility of remotely sensed CO₂ concentration data in surface source inversions. *Geophys. Res. Lett.*, **28**, 175-178.
- Rayner, P.J., D.M. O'Brien. 2001: The utility of remotely sensed CO₂ concentration data in surface source inversions. *Geophys. Res. Lett.*, **28**, 175-178.
- Rodgers, C. D., 1976: Retrieval of Atmospheric Temperature and Composition From Remote Measurements of Thermal Radiation. *Rev. Geophys. and Space Phys.*, **14**, 609-624.
- Rothman, L. S., C. P. Rinsland, A. Goldman, S. T. Massie, D. P. Edwards, J.-M. Flaud, A. Perrin, C. Camy-Peyret, V. Dana, J.-Y. Mandin, J. Schroeder, A. McCann, R. R. Gamache, R. B. Wattson, K. Yoshino, K. V. Chance, K. W. Jucks, L. R. Brown, V. Nemtchinov, and P. Varanasi, 1998: The HITRAN molecular spectroscopic database and HAWKS (HITRAN atmospheric workstation): 1996 edition, *J. Quant. Spectrosc. Radiat. Transfer*, **60**, 665-710.
- Saunders, R. W., M. Matricardi, and P. Brunel, 1999: An improved fast radiative transfer model for assimilation of satellite radiance observations. *Quart. J. Roy. Meteor. Soc.*, **125**, 1407-1425.
- Schimel, D., D. Alves, I. Enting, M. Heiman, F. Joos, D. Raynaud, T. Wigley, M. Prather, R. Derwent, D. Ehalt, P. Fraser, E. Sanhueza, X. Zhou, P. Jonas, R. Charlson, H. Rodhe, S. Sadasivan, K.P. Shine, Y. Fouquart, V. Ramaswamy, S. Solomon, J. Srinivasan, D. Albritton, R. Derwent, I. Isaksen, M. Lal and D. Wuebbles, 1995: Radiative Forcing of Climate Change. In: *Climate Change 1995, The Science of Climate Change*, J.T. Houghton, L.G.Meira Filho, B.A. Callander, N. Harris, A. Kattenberg and K. Maskell eds. Cambridge University Press, Cambridge, U.K., 69-131.



Scott, N.A., 1974: A direct method of computation of the transmission function of an inhomogeneous gaseous medium: description of the method and influence of various factors. *J. Quant. Spectrosc. Radiat. Transfer*, **14**, 691-707.

Scott, N.A., A. Chedin, 1981: A fast line-by-line method for atmospheric absorption computations: The Automated Atmospheric Absorption Atlas. *J. Appl. Meteor.*, **20**, 556-564.

Snyder, W.C., Z. Wan, Y. Zhang and Y.-Z. Feng, 1988: Classification-based emissivity for land surface temperature measurement from space. *Int. J. Remote Sensing*, **19**, 2753-2774.

Spencer, R. W. and J. R. Christy, 1993: Precision lower stratospheric temperature monitoring with the MSU: Validation and results 1979-1991. *J. Climate*, **6**, 1194-1204.

Strow, L.L., D.C Tobin and S.E. Hannon, 1994: A compilation of first-order line-mixing coefficients for CO₂ Q-branches. *J. Quant. Spectrosc. Radiat. Transfer*, **52**, 281.

Tans, P.P., I.Y. Fung and T. Takahashi, 1990: Observational constraints on the global atmospheric CO₂ budget. *Science*, **247**, 1431-1438.

Tournier, B., R. Armante and N.A. Scott, 1995: STRANSAC-93 et 4A-93: developpement et validation des nouvelles version des codes de transport radiatif pour application projet IASI. *Internal report LMD* no 201.

Trolier M., J.W.C. White, P.P. Tans, K.A. Masarie and P.A. Gemery, 1996: Monitoring the isotopic composition of atmospheric CO₂ : measurements from the NOAA global air sampling network, *J. Geophys. Res.*, **101** (D20), 25897-25916.

Turquety, S. J., J. Hadji-Lazaro, and C. Clerbaux, 2001: Retrieval of ozone from infrared IASI measurements. Passive infrared remote sensing of clouds and the atmosphere VI, *SPIE Proceedings Series* Int. Soc. Opt. Eng., to be published.

Wanninkhof, R., 1992: Relationship between wind speed and gas exchange over the ocean. *J. Geophys. Res.*, **97**, 7373-7382.

CO₂ concentration in the marine boundary layer
January 1, 1985 to January 1, 1994 (data source GLOBALVIEW-CO₂ 2000)

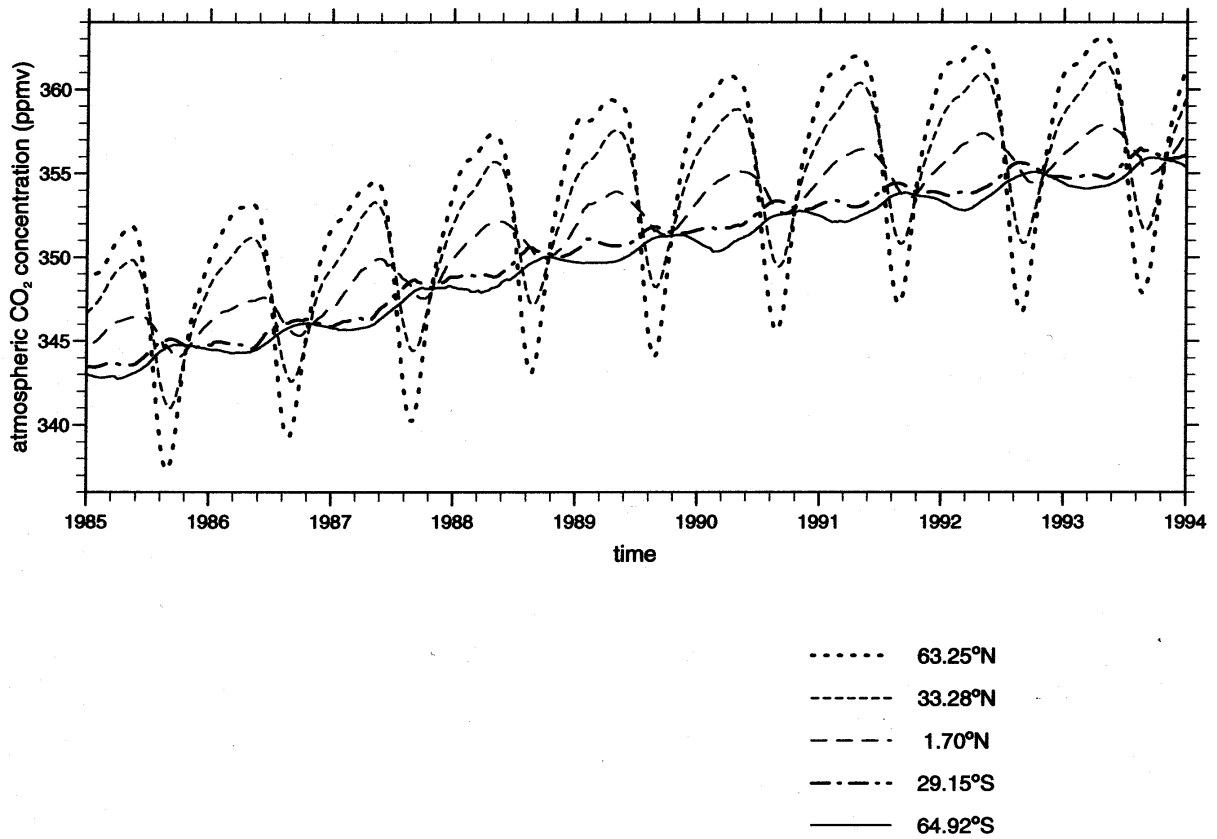


Fig 1: Evolution of atmospheric CO₂ concentrations from 1985 to 1994 at different latitudes (source GLOBALVIEW-CO₂, 2000).

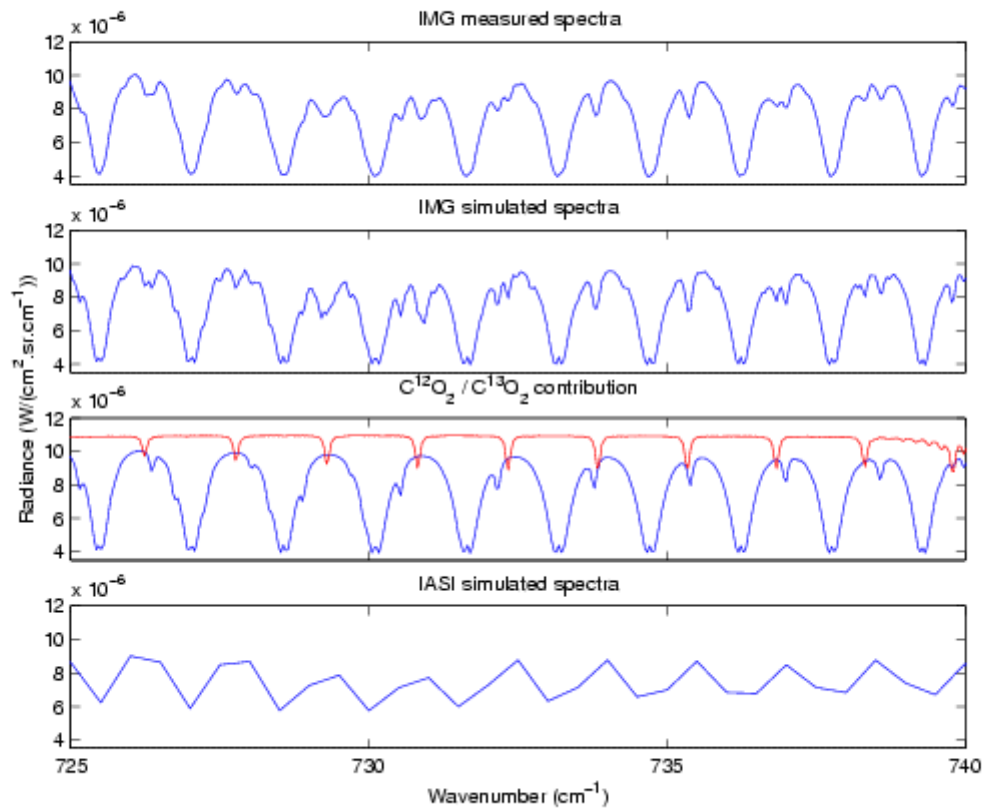


Fig 2: CO₂ absorption in the 725-740 cm⁻¹ spectral range. The panels show the IMG measured spectra, the IMG and IASI simulated spectra, and separated contributions from ¹²CO₂ and ¹³CO₂ respectively at the IMG spectral resolution.

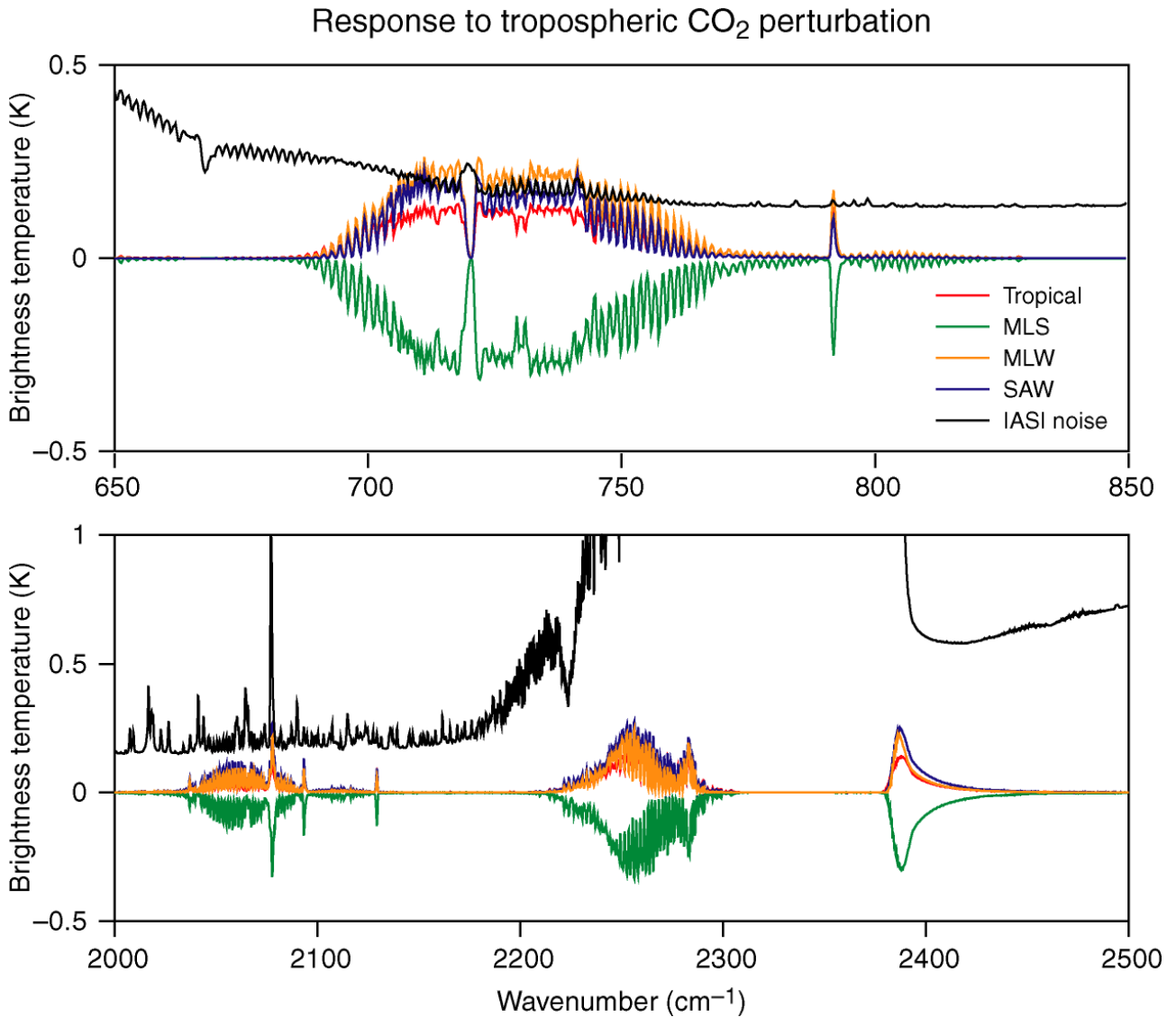


Fig 3: Response of simulated IASI radiance spectrum to changes in CO₂ concentration for 4 different standard atmospheres. The upper panel shows the response in the LW band and the lower panel the response in the SW band.

Response to temperature profile perturbation

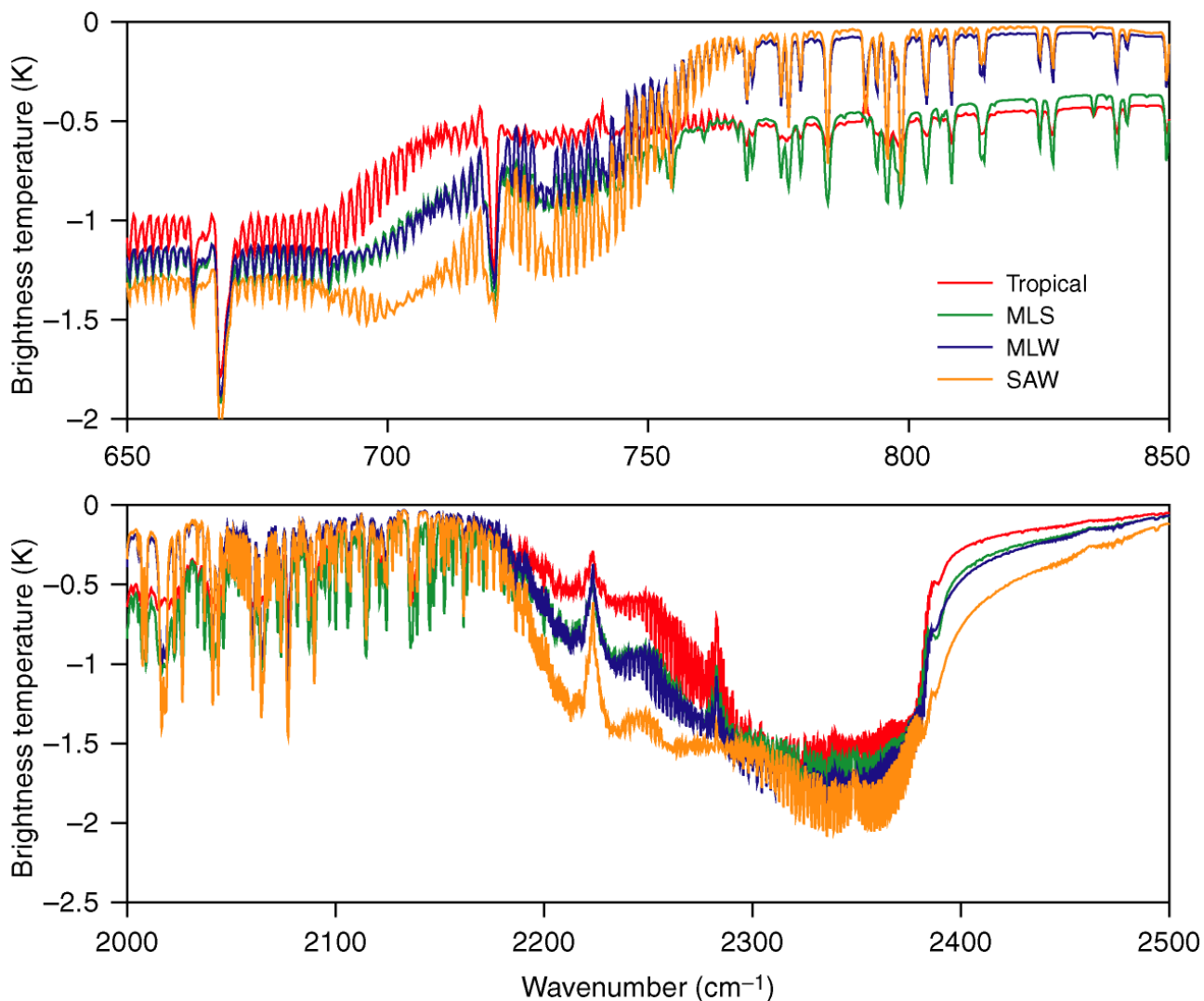


Fig 4: Response of IASI radiance spectrum to changes in temperature, equivalent to ECMWF background errors, for 4 different standard atmospheres. Note the surface temperature is modified by the same amount as the lowest atmospheric level.

Response to water vapour profile perturbation

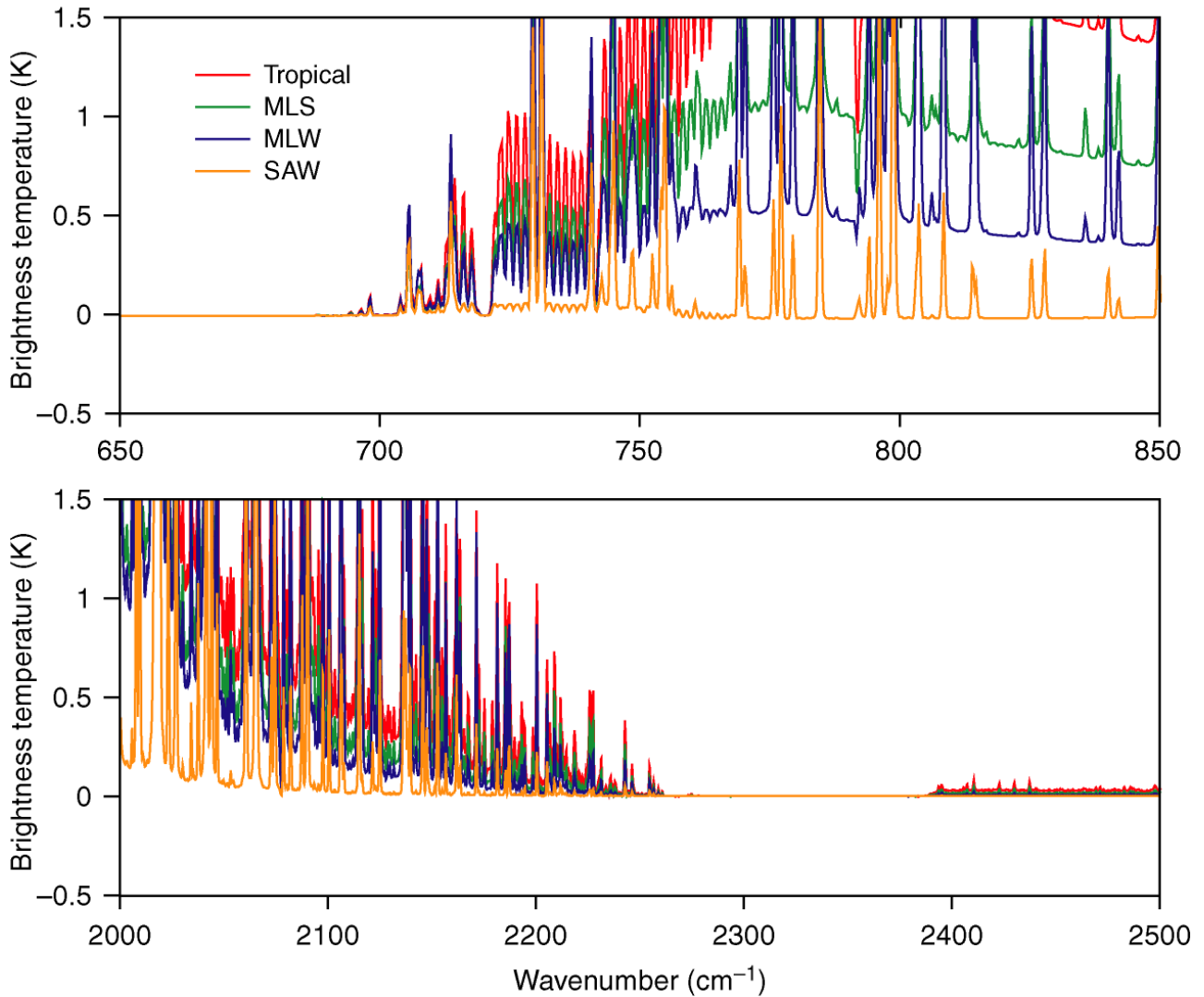


Fig 5: Response of IASI radiance spectrum to changes in water vapour concentration, equivalent to ECMWF background errors, for 4 different standard atmospheres.

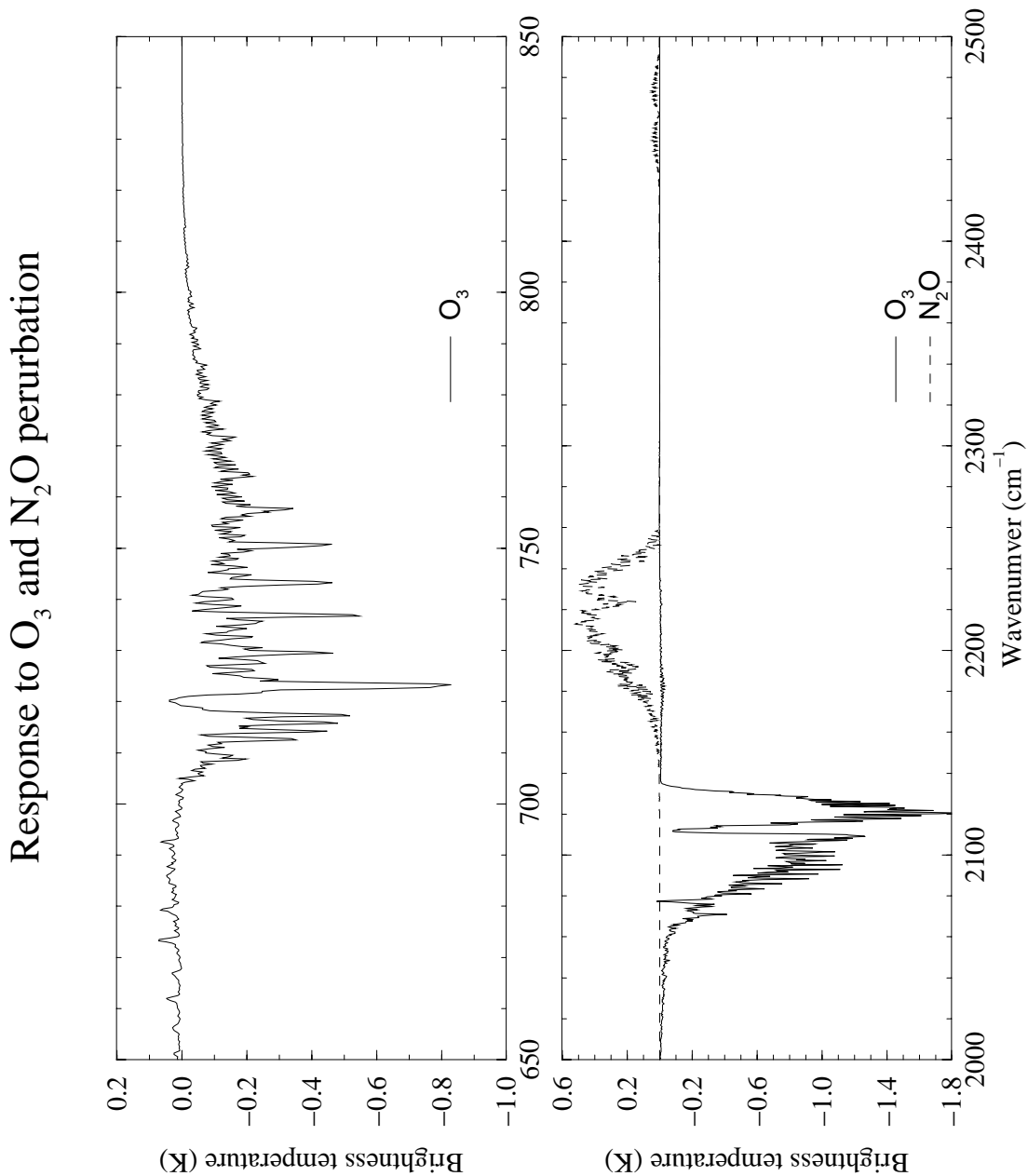


Fig 6: Response of IASI radiance spectrum to changes in ozone and nitrous oxide concentration (see text for perturbations).

Response to surface emissivity and surface temperature perturbation

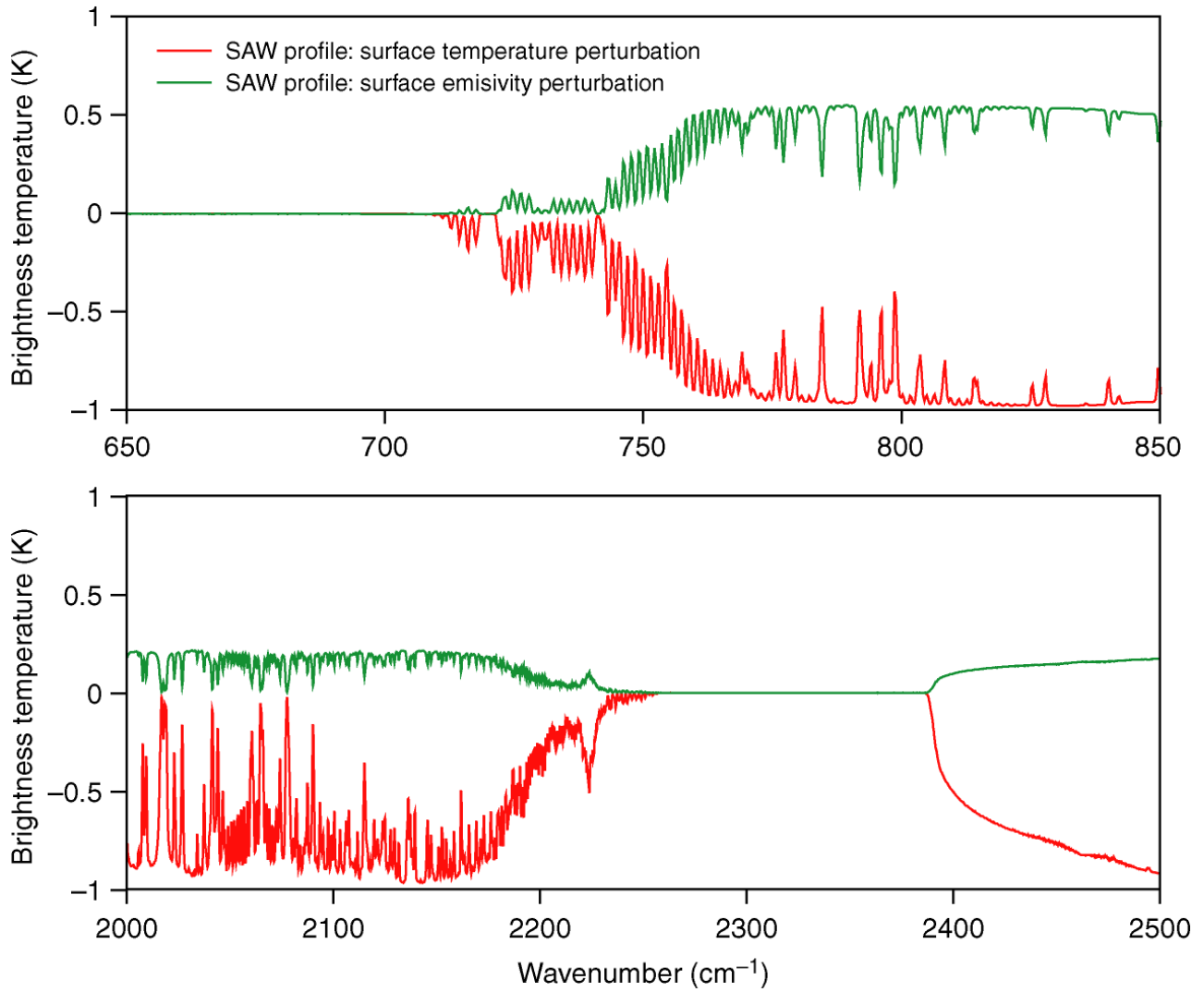


Fig 7: Response of IASI radiance spectrum to changes in only surface temperature or emissivity for the sub-arctic winter profile.

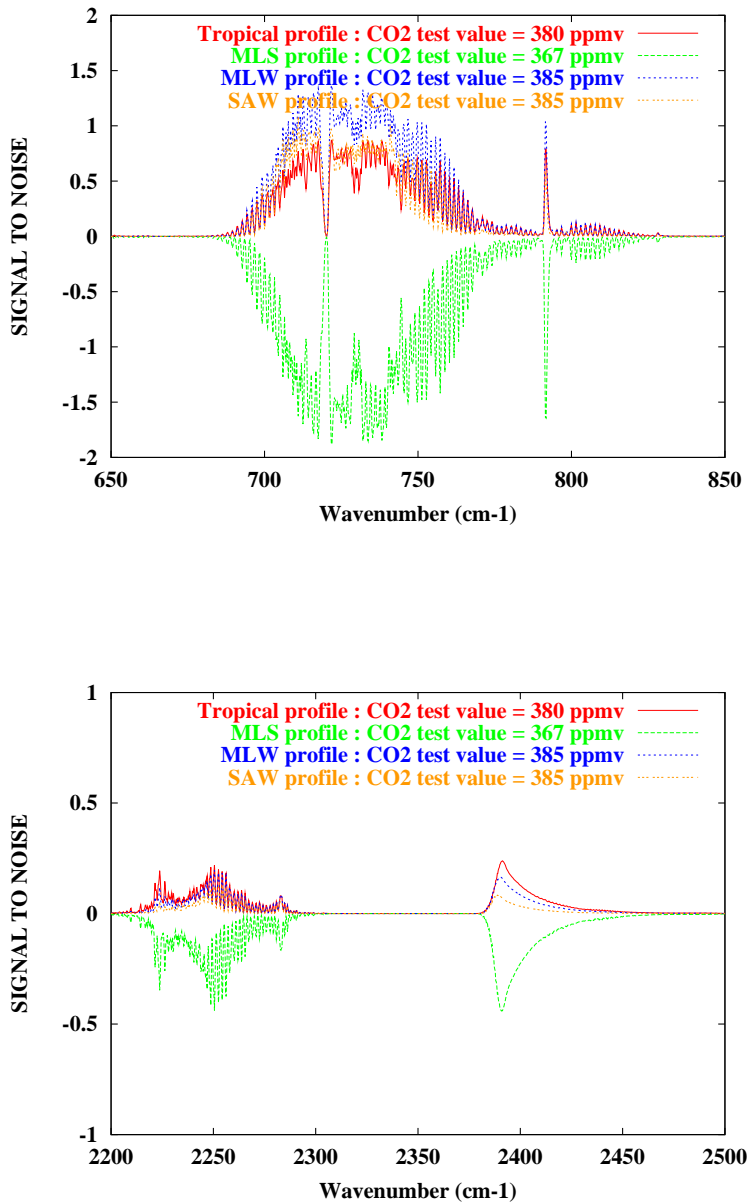


Fig 8: Signal (response of IASI to CO₂ changes) to noise (nominal IASI) ratio as a function of the wavenumber (cm⁻¹). Green: mid-latitude summer ; blue: mid-latitude winter ; red: tropical; orange: sub-arctic winter.

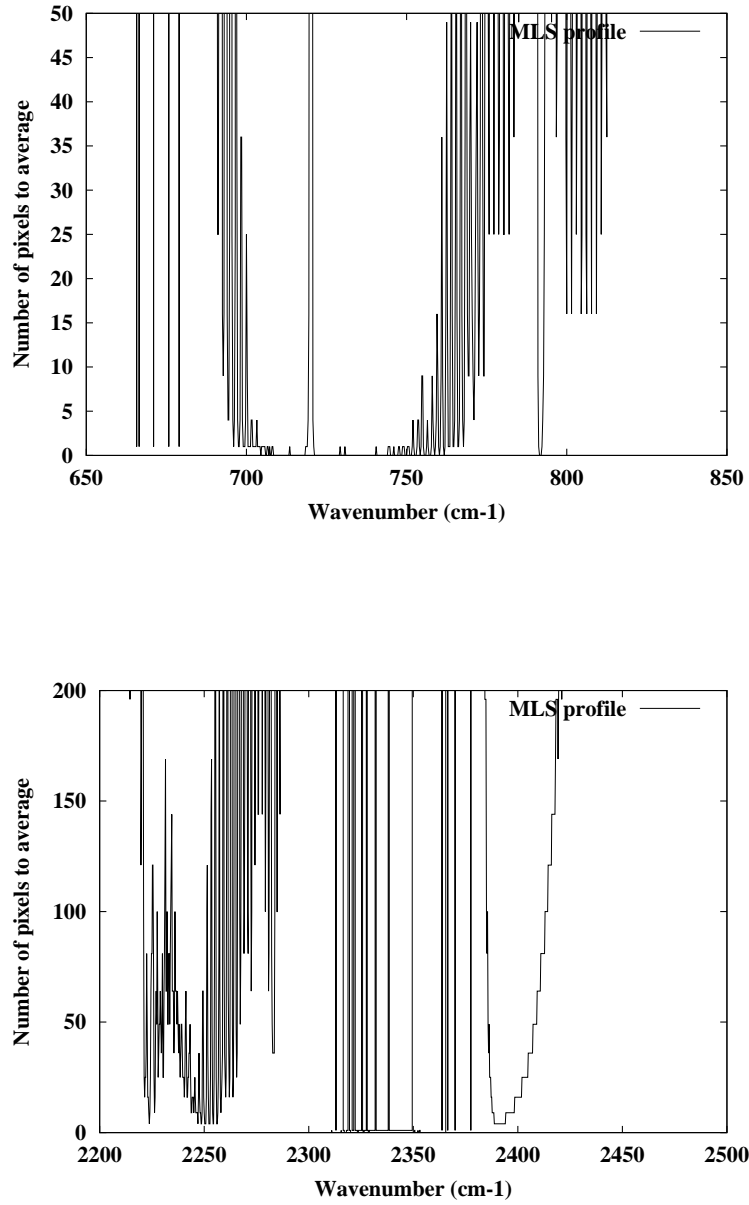


Fig 9: Number of IASI pixels to average to obtain a signal (CO_2 perturbation only) to noise ratio equal to 1 as a function of wavenumber (cm^{-1}).

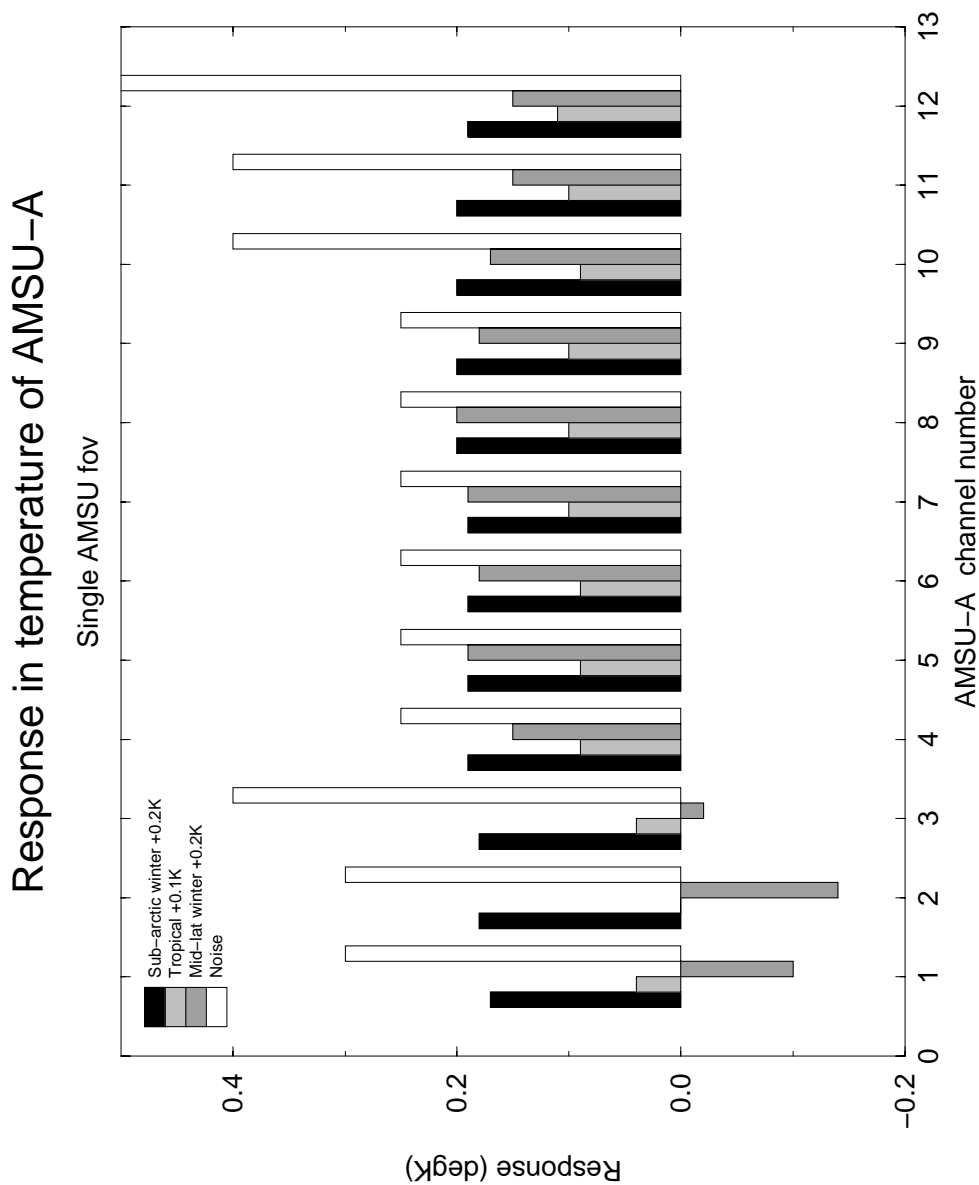


Fig 10: Response of AMSU-A channels to perturbations in temperature of the same order of magnitude as the CO₂ signal